AF4-ICP-MS as a powerful tool for the separation of gold nanorods and nanospheres

Sara López-Sanz [a], Nuria Rodríguez Fariñas [a], Mohammed Zougagh [b], Rosa del Carmen Rodríguez Martín-Doimeadios [a,*], Ángel Ríos [c,*]

[a] Department of Analytical Chemistry and Food Technology, Environmental Sciences Institute (ICAM), University of Castilla-La Mancha, Avda. Carlos III s/n, 45071 Toledo, Spain.

[b] Department of Analytical Chemistry and Food Technology, Faculty of Pharmacy, University of Castilla-La Mancha, Campus Universitario, 02071 Albacete, Spain.

[c] Department of Analytical Chemistry and Food Technology, Faculty of Chemical Sciences and Technologies, University of Castilla-La Mancha, Avda. Camilo José Cela s/n, 13071 Ciudad Real, Spain.

(*) Corresponding author:

Dr. Ángel Ríos Castro

E-mail: angel.rios@uclm.es

Dr. Rosa del Carmen Rodríguez Martín-Doimeadios

E-mail: rosacarmen.rodriguez@uclm.es

Abstract

An analytical methodology based on asymmetric flow field flow fractionation (AF4) hyphenated to inductively coupled plasma mass spectrometry (ICP-MS) has been developed to separate gold nanorods (AuNRs) and nanospheres (AuNSs). This separation is of special interest because the latter are the main impurity in the synthesis of AuNRs by seeding growth procedures, and quality control tools are highly demanded. AF4-ICP-MS separation was performed using a regenerated cellulose membrane (molecular weight cut-off, MWCO, of 10 kDa), a 350 μm thick spacer and a phosphate buffer (1 mM NaH_2PO_4, 1 mM Na_2HPO_4 at pH 7) with 0.01 % SDS as carrier. Several experimental parameters, such as focusing conditions and elution cross flow, and the injection/focusing time were optimized. Working under the optimum separation conditions, an adequate resolution was achieved between the void peak, commercially available AuNSs and AuNRs. The optimized method was successfully applied to the analysis of the products obtained in the synthesis procedure for AuNRs of 4.6 aspect ratio. Absorption molecular spectroscopy and transmission electron microscopy (TEM) have been used as complementary techniques.

Keywords

Gold nanoparticles; Nanospheres; Nanorods; Asymmetric flow field flow fractionation; Inductively coupled plasma mass spectrometry.

1. Introduction

Nowadays, gold nanoparticles (AuNPs) attract tremendous interest due to their unique properties (optical, electrochemical, magnetical, and catalytic), chemical stability and easy synthesis and functionalization [1]. Size, shape, composition and structure are the main characteristics that determine these properties. For instance, it is known that gold nanospheres (AuNSs) in aqueous solution exhibit an absorption peak from 500 to 550 nm [1], while octahedral- and triangle-shaped AuNPs show bands between 580 and 600 nm [2], and gold nanorods (AuNRs) present two bands in the visible and near infrared regions [3,4]. These properties lead to promising applications of AuNPs in different fields, such as sensing, imaging and biomedicine [1,3,5].

Among the AuNPs, the AuNRs are of special interest because they play a key role in very important biomedical applications, and both top-down and bottom-up synthesis procedures have been proposed [6,7]. Typical bottom-up methods include wet-chemical, electrochemical, sonochemical, solvothermal, microwave-assisted, and photochemical reduction techniques [4]. A hard or soft template, which serves to confine the growth along one direction, is required in these procedures and the most commonly used soft template is seeding-mediated growth [8]. AuNRs of different aspect ratio can be produced by working under controlled growth conditions following this approach [9,10]. Many efforts have been made to control the characteristics of the synthesized NPs but, unfortunately, a mixture in terms of particle sizes and shapes is obtained in many cases. The principal drawback associated with the seeded growth approach to AuNRs synthesis with controllable aspect ratio is the formation of spherical NPs of different size as side products, as well as, shorter rods and platelets[11]. The purification methods proposed are diverse with different potentials and limitations. The extraction and size selective precipitation methods allow separating AuNSs of different sizes but do not work for

AuNRs shape separation[12]. Nanoporous filter have been proposed for based shape separation but there are problems when the short axis of nanorods and spheres have the same diameter[11]. AuNRs can be separatd from small AuNSs by centrifugation but it is not suitable for similar sizes of rods, spheres, and platelets[13–15]. Moreover, it has been proposed a surfactant assisted self-assembly as AuNRs shape separation technique, where the centrifugation is used[11,16]. In this case, the experimental conditions such as concentration of the particle dispersion and a suitable particle stabilizer are very important to achieve the separation. However, different stages of precipitation and redispersion must be carried out to achieve an efficient separation and it is a very tedious methodology.. Therefore, it is necessary the development of purification procedures more efficient for the isolation of single size rods from a mixture of different rods and/or spheres. Moreover, it is also very important the quality control of the synthesis and purification procedures and they should be supported by appropriate analytical tools. [17].

For the characterization of NPs, electron microscopy, such as transmission electron microscopy (TEM) and scanning electron microscopy (SEM), among others, and some spectroscopic techniques, such as Raman and X-rays, have been traditionally used. However, all of them have different limitations mainly related to sample preparation, lack of reproducibility and low sensitivity [18,19]. An outstanding alternative recently proposed is the hyphenation of hydrodynamic separation techniques with sufficiently sensitive and selective detectors [20]. These techniques have been mainly used for the separation of AuNSs by size [21,22] and AuNRs like structured materials by aspect ratio [23–25] but, to the best of our knowledge, there are very few applications based on the separation by shape [26,27]. Size-exclusion chromatography [26], and capillary electrophoresis [27] were used with diode-array detection in both cases. Among hyphenated systems, the separation by asymmetric flow field flow fractionation (AF4) coupled to detection by inductively

coupled plasma mass spectrometry (ICP-MS) is particularly interesting because the advantages of AF4, in terms of resolving power and lack on interaction with the stationary phase, are combined with the high sensitivity and selectivity of ICP-MS [19,28–34]. In spite of the potential advantages, as far as we know, AF4-ICP-MS has never been used for the separation of different shapes of NPs with any detector.

The aim of this work is the development of an analytical strategy based on the use of AF4 coupled to ICP-MS to separate different AuNP shapes (AuNRs and AuNSs). The experimental parameters that affect the separation of the AuNSs and AuNRs will be optimized. The method will be applied for the quality control of the synthesis procedure of AuNRs.

2. Materials and methods

2.1 Materials

All chemicals and reagents were of analytical grade. Solutions were prepared in ultrapure water, which was obtained from Milli-Q® A10 TM water purification system (Millipore Corporation, USA). AuNSs stabilized in 0.2 mM citrate (11.3±0.9 nm and 20.0±2.5 nm) and AuNRs in water (69.3±10.1 nm x 12±0.8 nm, 5.79 aspect ratio, and 103.2±10.5 nm x 18.5±2.1 nm, 5.63 aspect ratio) were purchased from NanoComposix (USA). The concentrations of the commercial AuNSs, and AuNRs were estimated by quantification of the total gold content by ICP-MS [30]. The total gold concentrations were 51,886±2,183 ng mL^{-1} (n=3) and 43,638±135 ng mL^{-1} (n=3) for 10 nm and 20 nm AuNSs, respectively; and 6,768±80 ng mL^{-1} (n=3) and 4,322±56 ng mL^{-1} (n=3) for 5.79 and 5.63 aspect ratio AuNRs, respectively.

Rhodium, sodium dodecyl sulphate (SDS), $NaH_2PO_4.H_2O$ and $Na_2HPO_4.12H_2O$ were purchased from Inorganic Ventures (USA), Panreac (Spain) and Scharlab (Spain), respectively. Gold (III) chloride trihydrate ($HAuCl_4.3H_2O$), tri-sodium citrate ($Na_3C_6H_5O_7$), sodium tetrahydridoborate ($NaBH_4$), cetyltrimethylammonium bromide (CTAB), ascorbic acid ($C_6H_8O_6$) were purchased from Sigma-Aldrich (USA).

0.2 µm nylon filters (Agilent Technologies, Econofilter Nylon diameter 13 mm) and 0.1 µm membrane filters (Postnova, Germany) were used to filtrate the samples and the mobile phase, respectively.

2.2 Apparatus and instrumental features

The AF4 system was an AF2000 (Postnova Analytics, Germany). A membrane of regenerated cellulose (RC) with a molecular weight cut-off of 10 kDa was adapted as the accumulation wall. The trapezoidal channel was 27.5 cm in length and from 2 to 0.5 cm in width, and the spacer used was 350 µm thick. AF4 carrier solution was phosphate buffer (1 mM, pH 7) with the addition of SDS (0.01 %) and it was filtered through 0.1 µm membrane filters and degassed.

A Quadrupole ICP-MS Thermo X-SeriesII (Thermo Electron Corporation, Germany) equipped with a Meinhard nebulizer was employed. Rhodium (15 µg L^{-1}) was simultaneously aspirated during the ICP-MS data acquisition and it was applied to correct signal drifts. The raw data of the transient isotope signal for the different gold species and rhodium (internal standard) were exported from XSeries PlasmaLab software to OriginPro 2016 software, where they were processed.

A spectrophotometer (model UV-3600, Shimadzu, Japan) was used to record spectra at room temperature in the 190-1400 nm range, with resolution of 1 nm and 0.1 cm path length quartz cuvettes.

TEM images were acquired on a JEOL JEM 1400 operating at an acceleration voltage of 80 kV. Samples were prepared by drying a drop of 10 µL on a carbon-coated copper grid.

An advanced vortex mixer (Velp Scientifica, ZX3, Italy) was used to prepare samples.

2.3 Procedure for the synthesis of 4.6 aspect ratio AuNRs

The 4.6 aspect ratio AuNRs were synthesized according to Jana et al. [9]. Briefly, a seed solution (3.5 nm AuNSs) was prepared from 20 mL of a mixture of 2.5×10^{-4} M $HAuCl_4$ and 2.5×10^{-4} M tri-sodium citrate, and 0.6 mL of ice cold 0.1 M $NaBH_4$ solution in a conical flask under stirring. This seed solution was used within 2-5 h after preparation. In a clean test tube, 10 mL of a growth solution (2.5×10^{-4} M $HAuCl_4$ and 0.1 M CTAB) was mixed with 0.05 mL of 0.1 M ascorbic acid. Finally, 0.025 mL of the seed solution was added to the test tube, and after 5-10 min, the 4.6 aspect ratio AuNRs are ready.

3. Results and discussion

3.1 Optimization of the AF4-ICP-MS method

Based on previous studies about AuNPs, a regenerated cellulose membrane (MWCO of 10 KDa) and a 350 µm thick spacer were used [31]. When a membrane is used

for the first time, it is common to do a pre-conditioning to avoid undesirable membrane-particle interactions [35,36]. In our case, five consecutive injections of AuNSs were enough for conditioning the new membrane. Moreover, according to the literature, a phosphate buffer (1 mM NaH_2PO_4, 1 mM Na_2HPO_4 at pH 7) with the addition of 0.01 % SDS could be appropriate as mobile phase for several reasons. The presence of monovalent cations in the carrier can avoid the formation of aggregates and has no effect on the fractionation times [37]; a correct selection of pH reduces the loss of particulate material by adsorption on the membrane and avoids electrostatic attraction between the NPs and the membrane [32]; and the addition of surfactants to the mobile phase increases the NPs stability and contributes to minimize the possible aggregation or adsorption [33].

Once the dimensions of the channel, the type of membrane and the carrier composition were selected, it was necessary to optimize several experimental parameters related to the AF4 system, such as the focusing conditions and elution cross flow, and injection/focusing time. A sample of 20 nm AuNSs (87 ng mL^{-1}) and 5.63 aspect ratio AuNRs (104 ng mL^{-1}) prepared in the carrier solution from AuNPs commercially available was used in the optimization study.

One of the most important variables that affect the fractionation of NPs by AF4 is the cross flow. The smallest particles require a great flow to be separated properly. However, high flow rates lead to longer fractionation times and selective losses of the largest particles in the sample. One option for samples with a wide range of particle size is to apply gradients, that is, to reduce the cross flow over time. Therefore, different gradients of the cross flow were evaluated and they are shown in Table S1. The injection flow (0.20 mL min^{-1}), injection time (5 min) and cross and focus flow (0.50 and 0.80 mL min^{-1}, respectively) were kept constant in the focusing step. The programs of gradient A, B and C (Table S1) did not facilitatethe separation (Figure S1, S2, and S3). However, the

use of a gradient cross flow starting at 0.5 mL min^{-1} followed by a power decay (exponent 1.5) for longer times (45 min) (Table 1) resulted in an appropriate separation between the void peak (first peak, 7.5 min) and that of the 20 nm AuNSs (second peak, 13.5 min), and between this and 5.63 aspect ratio AuNRs (third peak, 23 min) (Figure 1). The fraction of void peak could be due to a possible "memory effect" because of a release of NPs during carrier injection or the presence of a small particles fraction in the AuNPs commercially available [34]. In order to evaluate if the injection time has an effect on the separation of NPs, the injection/focusing time was modified from 2.5 to 7.5 min. As illustrated in Figure S4, longer injection times produced a shift to longer fractionation times and a decrease in the fraction of void peak. Besides, it was observed that the intensity of AuNSs and AuNRs peaks was high for an injection time of 5 min, so it was selected for further experiments (Table 1).

The AF4 theory can be used to estimate the hydrodynamic diameters of the AuNSs and AuNRs from their retention times in the fractograms (Figure 1). The retention time of the AuNSs (13.5 min) can be related to the diffusion coefficient according to Runyon et al. equation ($t_r=(w^2/6D)*\ln(1+(V_c/V))$, retention time ($t_r$), channel thickness (w), diffusion coefficient (D), cross flow rate (V_c), and flow rate exiting through the channel outlet (V)) [25], and subsequently to the hydrodynamic diameter (Stokes-Einstein equation: $d_h=kT/3\pi\eta D$, hydrodynamic diameters (d_h), Boltzmann constant ($k=1.38x10^{-23}$ $kgm^2s^{-2}K^{-1}$), temperature (T), viscosity ($\eta=0.000891$ $kgm^{-1}s^{-1}$), and diffusion coefficient (D)), which was 28 nm. However, Beckett et al. established that the retention time does not depend only on the diffusion coefficient, since a certain dependence of the shape would be expected [38]. In the case of AuNRs, the retention time (23 min) is principally dependent on the translational diffusion coefficient (not of the rotational diffusion coefficient) [25], which can be determined according to the El Hadri et al. equation ($D_{t\text{-}AF4}=V_c w^2 t_0/12V_0 t_r$,

translational diffusion coefficient (D_t), cross flow rate (V_c), channel thickness (w), void time (t_0), void volume (V_0), and retention time (tr)) [23]. Using the Stokes-Einstein equation and taking into account that D_t corresponding to the cylinder model (aspect ratio between 2 to 20) equals the D [23]. The equivalent sphere diameter for the AuNRs was 66.3 nm. As expected, the hydrodynamic diameter of the AuNRs (66.3 nm) is greater than the AuNSs (28 nm) and this justifies the separation found by AF4.

Several experiments with AuNRs of different aspect ratios (5.63 and 5.79) and AuNSs of different sizes (10 and 20 nm), were carried out to demonstrate the strength of the method as a whole. As illustrated in Figure S5, the separations were satisfactory and the retention times changed with different aspect ratios (Figure S5, black line *versus* grey line) and sizes (Figure 1 *versus* Figure S5). Besides, different concentrations of 10 nm AuNSs (27, 54, 108, and 216 ng mL^{-1}) were spiked to samples containing 5.63 aspect ratio AuNRs (60 ng mL^{-1}). The samples were analysed and their fractograms are shown in Figure 2. It was possible to verify that the intensity of the AuNRs peak remained constant while the intensity of the AuNSs peak increased. This demonstrates the feasibility of the proposed method to separate mixtures of AuNRs and AuNSs at different concentration ratios.

3.2. Study by AF4-ICP-MS and complementary techniques of AuNRs synthesis procedure

The optimized AF4-ICP-MS method will be used for the quality control of products obtained after the synthesis of 4.6 aspect ratio AuNRs using a seeding growth method [9]. Samples (dilution 1/100) obtained in the synthesis were analyzed and a fractogram is shown in Figure 3a. A first peak (7.5 min) corresponding to the fractionation time of the void peak is observed (Figure 3a). Its high intensity could be related to

impurities of the synthesis procedure, maybe small AuNSs (3.5 nm or lesser) of the seed solution.

The second peak (Figure 3a) at 19 min (estimated diameter of 54.7 nm) is close to the AuNRs commercially available with an aspect ratio of 5.63 (Figure 1). This peak corresponds to the expected dimensions of the AuNPs according to the synthesis conditions and the low intensity could indicate that the yield was limited. The response factor method was used to quantify the concentration of AuNRs from the peak area in the registered fractogram. The 5.63 aspect ratio AuNRs commercial solution (104 ng mL^{-1}) was the reference selected for the quantification. The estimated concentration of the AuNRs in the synthesized sample was 3,400 ng mL^{-1}.

Moreover, it is necessary to know the fractionation time and intensity of the AuNPs commercially available in the synthesis medium for an adequate comparison. Therefore, samples obtained in the synthesis procedure were spiked independently with commercially available 20 nm AuNSs (873 ng mL^{-1}) or 5.63 aspect ratio AuNRs (1,040 ng mL^{-1}), and they were analyzed (Figure 3b). The fractionation times of the commercially available AuNPs spiked (Figure 3b) were similar to those previously obtained in the carrier solution (Figure 1). This fact confirms that the fractionation times do not change in the synthesis medium and that the second peak found in the Figure 3a could be the 4.6 aspect ratio AuNRs similar to the commercially available AuNRs (5.63 aspect ratio). However, the intensity of the commercially available AuNPs in the synthesis medium are lower than the expected. Low recovery values cannot be attributed to undesirable membrane-particle interactions because the membrane had been previously stabilized and will be further investigated using the information given in the fractograms.

The third peak (Figure 3a) at 57.5 min represents AuNRs with an aspect ratio greater than 5.63 or aggregates/agglomerates of AuNPs, which was not expected according to the used synthesis. When the samples obtained in the synthesis procedure were spiked independently with both commercially available AuNPs (Figure 3b), the intensity of the second peak was lower than expected, while the third peak was even higher than in Figure 3a. These changes could indicate the possible formation of aggregates/agglomerates of NPs.

The different spectroscopic absorption characteristics of the AuNSs and AuNRs were exploited to get a closer insight into these processes. The absorption spectra of a sample from the synthesis procedure of 4.6 aspect ratio AuNRs, as well as the commercially available AuNSs and AuNRs were recorded (Figure 4). As expected, the commercially available 20 nm AuNSs has an absorption maximum at 500 nm (Figure 4, grey line), while the commercially available 5.63 aspect ratio AuNRs has two, the first one at 500 nm and the second one at 950 nm (Figure 4, dash line). However, the sample from the synthesis has a major band at 500 nm (Figure 4, black line). This band indicate the presence of AuNSs, probably as impurities of the seed solution in the synthesis procedure. Moreover, the lack of a major band in the near-infrared region indicates that there is not a significant amount of AuNRs. These results agree with those previously reported by AF4-ICP-MS (Figure 3a).

In addition, the TEM analysis of the sample from the synthesis procedure of 4.6 aspect ratio AuNRs (dilution 1/100) was carried out (Figure 5). A mixture of AuNRs of different aspect ratios, AuNSs and other shapes, was found. The TEM image confirmed the existence of AuNRs with the expected aspect ratio and also showed the presence of other much higher ones, which confirms the information obtained by AF4-ICP-MS. However, the TEM image cannot show the existence of small AuNSs (3.5 nm or lesser)

of the seed solution, probably, because the size is too small to be detected by the instrument used.

Problems related to the synthesis procedure for small AuNRs (4.6 aspect ratio) and difficulties for purification have been also reported by other authors [9]. Therefore, it is very important to perform an adequate quality control and the developed method based on AF4-ICP-MS has demonstrated its capability for this purpose. Moreover, AF4 can be useful in the fractional collection mode to separate the particle mixture into monodisperse NPs. This approach has been already used by Runyon et al. to separate AuNRs of different aspect ratio using AF4-UV-vis. Moreover, they collected the fractions which were analyzed by UV-vis and TEM, and one of them was a mixture of AuNRs and AuNSs [25]. Therefore, this potential should be explored in further studies for purification and quality control.

4. Conclusions

A methodology based on AF4 hyphenated to ICP-MS has been proposed to separate AuNPs of different shapes, namely AuNSs and AuNRs. After the optimization of the adequate separation conditions, its applicability for quality control of synthesis procedures of AuNRs has been demonstrated. In combination with UV-vis molecular absorption spectroscopy and TEM as complementary techniques, the presence of significant impurities has been pointed out.

The development of hyphenated techniques, such as the proposed in this work, for the separation of NPs by shape is of major interest because this characteristic is very important for their applications in different fields. Further experiments should be carried out to evaluate the capabilities of this approach as a tool for purification purposes.

Acknowledgments

The authors would like to thank the Ministerio de Economía y Competitividad (MINECO) for financial support through the project CTQ2016-78793-P, as well as the pre-doctoral contract, BES-2014-069095. Junta de Comunidades de Castilla – La Mancha is also acknowledged by funding through SBPLY/17/180501/000626 Grant. The AEI/FEDER-UE is thanked for the finantial support (UNCM 13-1E-1565) for the adquisition of the AF4 system.

Supplementary Material

Supplementary data associated with this article is provided.

References

1 Y.-C. Yeh, B. Creran and V. M. Rotello, *Nanoscale*, 2012, **4**, 1871–1880.

2 M. A. Casado-Rodriguez, M. Sanchez-Molina, A. Lucena-Serrano, C. Lucena-Serrano, B. Rodriguez-Gonzalez, M. Algarra, A. Diaz, M. Valpuesta, J. M. Lopez-Romero, J. Perez-Juste and R. Contreras-Caceres, *Nanoscale*, 2016, **8**, 4557–4564.

3 N. Li, P. Zhao and D. Astruc, *Angew. Chemie Int. Ed.*, 2014, **53**, 1756–1789.

4 H. Chen, L. Shao, Q. Li and J. Wang, *Chem. Soc. Rev.*, 2013, **42**, 2679–2724.

5 N. Elahi, M. Kamali and M. H. Baghersad, *Talanta*, 2018, **184**, 537–556.

6 N. Li, D. Niu, X. Jia, J. He, Y. Jiang, J. Gu, Z. Li, S. Xu and Y. Li, *J. Mater. Chem. B*, 2017, **5**, 1642–1649.

7 J. Zhou, Z. Cao, N. Panwar, R. Hu, X. Wang, J. Qu, S. C. Tjin, G. Xu and K. T. Yong, *Coord. Chem. Rev.*, 2017, **352**, 15–66.

8 A. Gole and C. J. Murphy, *Chem. Mater.*, 2004, **16**, 3633–3640.

9 N. R. Jana, L. Gearheart and C. J. Murphy, *J. Phys. Chem. B*, 2001, **105**, 4065–4067.

10 B. Nikoobakht and M. A. El-Sayed, *Chem. Mater.*, 2003, **15**, 1957–1962.

11 N. R. Jana, *Chem. Commun.*, 2003, **9**, 1950.

12 H. Yao, O. Momozawa, T. Hamatani and K. Kimura, *Chem. Mater.*, 2001, **13**, 4692–4697.

13 N. R. Jana, L. Gearheart and C. J. Murphy, *Chem. Commun.*, 2001, 617–618.

14 N. R. Jana, L. Gearheart and C. J. Murphy, *Adv. Mater.*, 2001, **13**, 1389–1393.

15 C. J. Murphy and N. R. Jana, Controlling the Aspect Ratio of Inorganic Nanorods and Nanowires.

16 S. E. Lohse and C. J. Murphy, *Chem. Mater.*, 2013, **25**, 1250–1261.

17 S. López-Sanz, F. J. Guzmán Bernardo, R. C. Rodríguez Martín-Doimeadios and Á. Ríos, *Anal. Chim. Acta*, 2019, **1059**, 1–15.

18 P.-C. Lin, S. Lin, P. C. Wang and R. Sridhar, *Biotechnol. Adv.*, 2014, **32**, 711–726.

19 F. Laborda, E. Bolea, G. Cepriá, M. T. Gómez, M. S. Jiménez, J. Pérez-Arantegui and J. R. Castillo, *Anal. Chim. Acta*, 2016, **904**, 10–32.

20 A. Lapresta-Fernández, A. Salinas-Castillo, S. Anderson de la Llana, J. M. Costa-Fernández, S. Domínguez-Meister, R. Cecchini, L. F. Capitán-Vallvey, M. C. Moreno-Bondi, M.-P. Marco, J. C. Sánchez-López and I. S. Anderson, *Crit. Rev. Solid State Mater. Sci.*, 2014, **39**, 423–458.

21 M. Bouri, R. Salghi, M. Algarra, M. Zougagh and A. Ríos, *RSC Adv.*, 2015, **5**, 16672–16677.

22 S. López-Sanz, N. R. Fariñas, R. S. Vargas, R. del C. R. Martín-Doimeadios and Á. Ríos, *Talanta*, 2017, **164**, 451–457.

23 H. El Hadri, J. Gigault, J. Tan and V. A. Hackley, *Anal. Bioanal. Chem.*, 2018, **410**, 6977–6984.

24 J. Gigault, T. J. Cho, R. I. MacCuspie and V. A. Hackley, *Anal. Bioanal. Chem.*, 2013, **405**, 1191–1202.

25 J. R. Runyon, A. Goering, K.-T. Yong and S. K. R. Williams, *Anal. Chem.*, 2013, **85**, 940–948.

26 G.-T. Wei, F.-K. Liu and C. R. C. Wang, *Anal. Chem.*, 1999, **71**, 2085–2091.

27 C. Adelantado, M. Algarra, M. Zougagh and Á. Ríos, *Electrophoresis*, 2018, **39**, 1437–1442.

28 B. Meermann, *Anal. Bioanal. Chem.*, 2015, **407**, 2665–2674.

29 L. Sánchez-García, E. Bolea, F. Laborda, C. Cubel, P. Ferrer, D. Gianolio, I. da Silva and J. R. Castillo, *J. Chromatogr. A*, 2016, **1438**, 205–15.

30 S. López-Sanz, N. R. Fariñas, R. del C. R. Martín-Doimeadios and Á. Ríos, *Anal. Chim. Acta*, 2019, **1053**, 178–185.

31 B. Meisterjahn, E. Neubauer, F. Von der Kammer, D. Hennecke and T. Hofmann, *J. Chromatogr. A*, 2014, **1372C**, 204–211.

32 O. Geiss, C. Cascio, D. Gilliland, F. Franchini and J. Barrero-Moreno, *J. Chromatogr. A*, 2013, **1321**, 100–108.

33 K. Ramos, L. Ramos, C. Cámara and M. M. Gómez-Gómez, *J. Chromatogr. A*, 2014, **1371**, 227–36.

34 I. López-Heras, Y. Madrid and C. Cámara, *Talanta*, 2014, **124**, 71–78.

35 B. Schmidt, K. Loeschner, N. Hadrup, A. Mortensen, J. J. Sloth, C. Bender Koch and E. H. Larsen, *Anal. Chem.*, 2011, **83**, 2461–2468.

36 A. Ulrich, S. Losert, N. Bendixen, A. Al-Kattan, H. Hagendorfer, B. Nowack, C. Adlhart, J. Ebert, M. Lattuada and K. Hungerbühler, *J. Anal. At. Spectrom.*, 2012, **27**, 1120.

37 S. Dubascoux, F. Von Der Kammer, I. Le Hécho, M. P. Gautier and G. Lespes, *J. Chromatogr. A*, 2008, **1206**, 160–165.

38 R. Beckett and J. C. Giddings, *J. Colloid Interface Sci.*, 1997, **186**, 53–59.

Legends to figures

Figure 1. AF4-ICP-MS fractogram of a mixture containing commercially available 20 nm AuNSs (87 ng mL^{-1}) and 5.63 aspect ratio AuNRs (104 ng mL^{-1}). Optimal cross flow program Table 1 (dash line). Carrier: 0.01 % SDS, 1 mM NaH_2PO_4, 1 mM Na_2HPO_4, pH 7.

Figure 2. AF4-ICP-MS fractogram of a mixture containing commercially available 10 nm AuNSs at different concentrations: 27 ng mL^{-1} (black line), 54 ng mL^{-1} (grey line), 108 ng mL^{-1} (black dash line), and 216 ng mL^{-1} (grey dash line), and 5.63 aspect ratio AuNRs (60 ng mL^{-1}). Optimal cross flow program Table 1. Carrier: 0.01 % SDS, 1 mM NaH_2PO_4, 1 mM Na_2HPO_4, pH 7.

Figure 3. AF4-ICP-MS fractograms of a sample obtained in the synthesis procedure of 4.6 aspect ratio AuNRs (dilution 1/100): a) directly, b) spiked with commercially available 20 nm AuNSs (873 ng mL^{-1}) (grey line) or with 5.63 aspect ratio AuNRs (1,040 ng mL^{-1}) (dash line). Optimal cross flow program Table 1. Carrier: 0.01 % SDS, 1 mM NaH_2PO_4, 1 mM Na_2HPO_4, pH 7.

Figure 4. Absorption spectra of a sample obtained in the synthesis procedure of 4.6 aspect ratio AuNRs (black line), the commercially available 20 nm AuNSs (43,638 ng mL^{-1}) (grey line) and 5.63 aspect ratio AuNRs (4,332 ng mL^{-1}) (dash line).

Figure 5. TEM image of a sample obtained in the synthesis procedure of 4.6 aspect ratio AuNRs (dilution 1/100).

Table 1. Optimum instrumental conditions for the AF4-ICP-MS system.

AF4				
	Channel thickness (μm)	350		
	Membrane type	Regenerated cellulose; cut-off, 10 kDa		
	Injection loop (μL)	50		
	Carrier liquid composition	0.01 % SDS, 1mM NaH_2PO_4, 1mM Na_2HPO_4, pH 7		
	Focus flow (mL min^{-1})	0.8		
	Detector flow (mL min^{-1})	0.5		
	Cross flow program	Time (min)	Regime	Cross flow (mL min^{-1})
	Injection/focusing	5	Injection flow, 0.2 mL min^{-1}	0.5
	Elution cross flow	45	Power (Exponent 1.5)	0.5 to 0
		10	Constant	0
ICP-MS				
	RF-Power (KW)	1.4		
	Plasma gas flow rate (L min^{-1})	15		
	Carrier gas flow rate (L min^{-1})	0.98		
	Nebulizer flow rate (L min^{-1})	0.9		
	Auxiliary gas flow rate (L min^{-1})	1		
	Spray chamber	Scott type		
	Isotopes monitored	^{197}Au, ^{103}Rh		
	Dwell time (ms)	100		

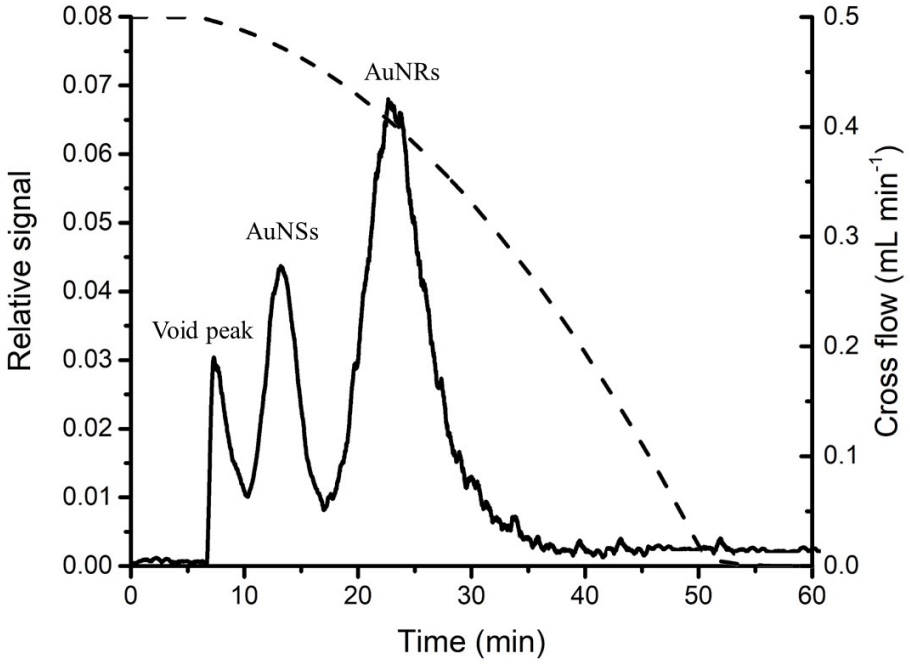

Figure 1. AF4-ICP-MS fractogram of a mixture containing commercially available 20 nm AuNSs (87 ng mL-1) and 5.63 aspect ratio AuNRs (104 ng mL-1). Optimal cross flow program Table 1 (dash line). Carrier: 0.01 % SDS, 1 mM NaH2PO4, 1 mM Na2HPO4, pH 7.

249x190mm (120 x 120 DPI)

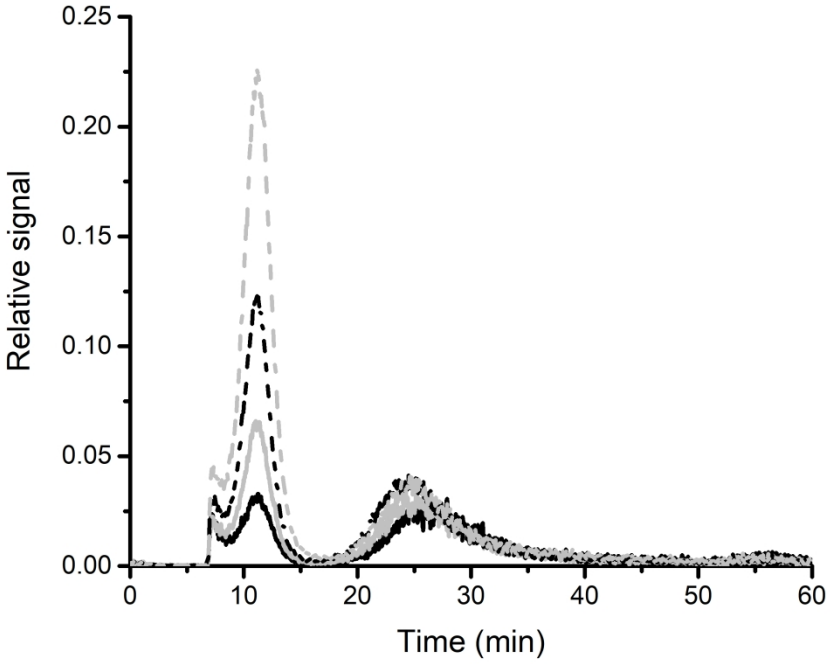

Figure 2. AF4-ICP-MS fractogram of a mixture containing commercially available 10 nm AuNSs at different concentrations: 27 ng mL-1 (black line), 54 ng mL-1 (grey line), 108 ng mL-1 (black dash line), and 216 ng mL-1 (grey dash line), and 5.63 aspect ratio AuNRs (60 ng mL-1). Optimal cross flow program Table 1. Carrier: 0.01 % SDS, 1 mM NaH_2PO_4, 1 mM Na_2HPO_4, pH 7.

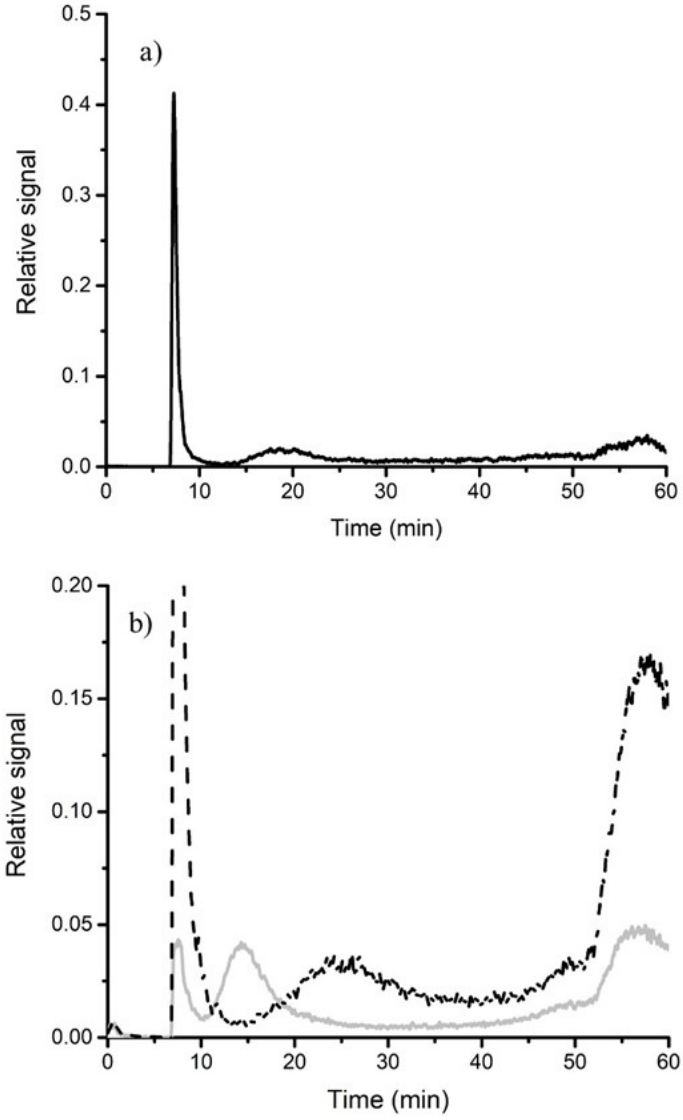

Figure 3. AF4-ICP-MS fractograms of a sample obtained in the synthesis procedure of 4.6 aspect ratio AuNRs (dilution 1/100): a) directly, b) spiked with commercially available 20 nm AuNSs (873 ng mL-1) (grey line) or with 5.63 aspect ratio AuNRs (1,040 ng mL-1) (dash line). Optimal cross flow program Table 1. Carrier: 0.01 % SDS, 1 mM NaH2PO4, 1 mM Na2HPO4, pH 7.

131x190mm (120 x 120 DPI)

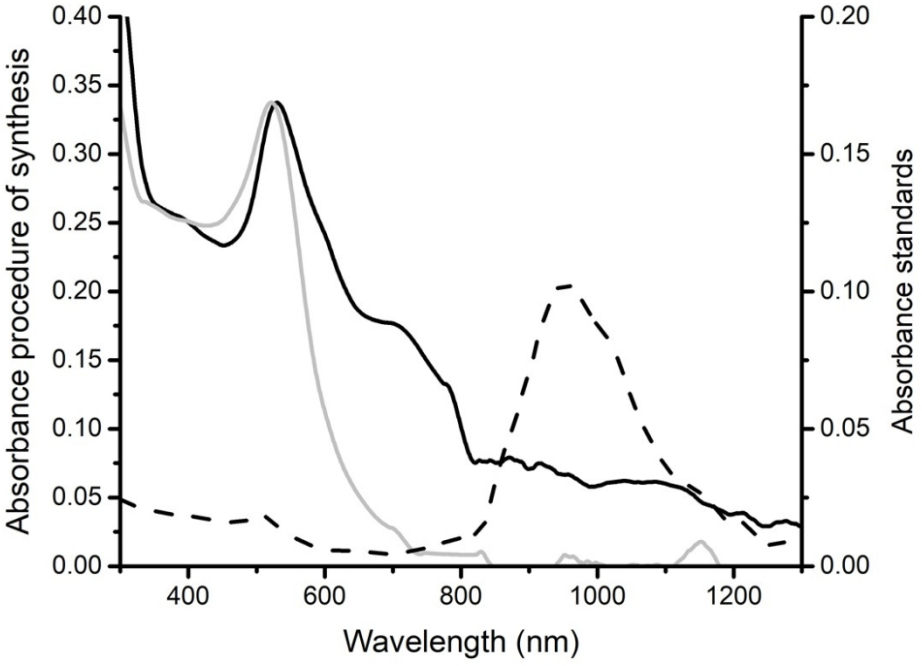

Figure 4. Absorption spectra of a sample obtained in the synthesis procedure of 4.6 aspect ratio AuNRs (black line), the commercially available 20 nm AuNSs (43,638 ng mL-1) (grey line) and 5.63 aspect ratio AuNRs (4,332 ng mL-1) (dash line).

248x190mm (120 x 120 DPI)

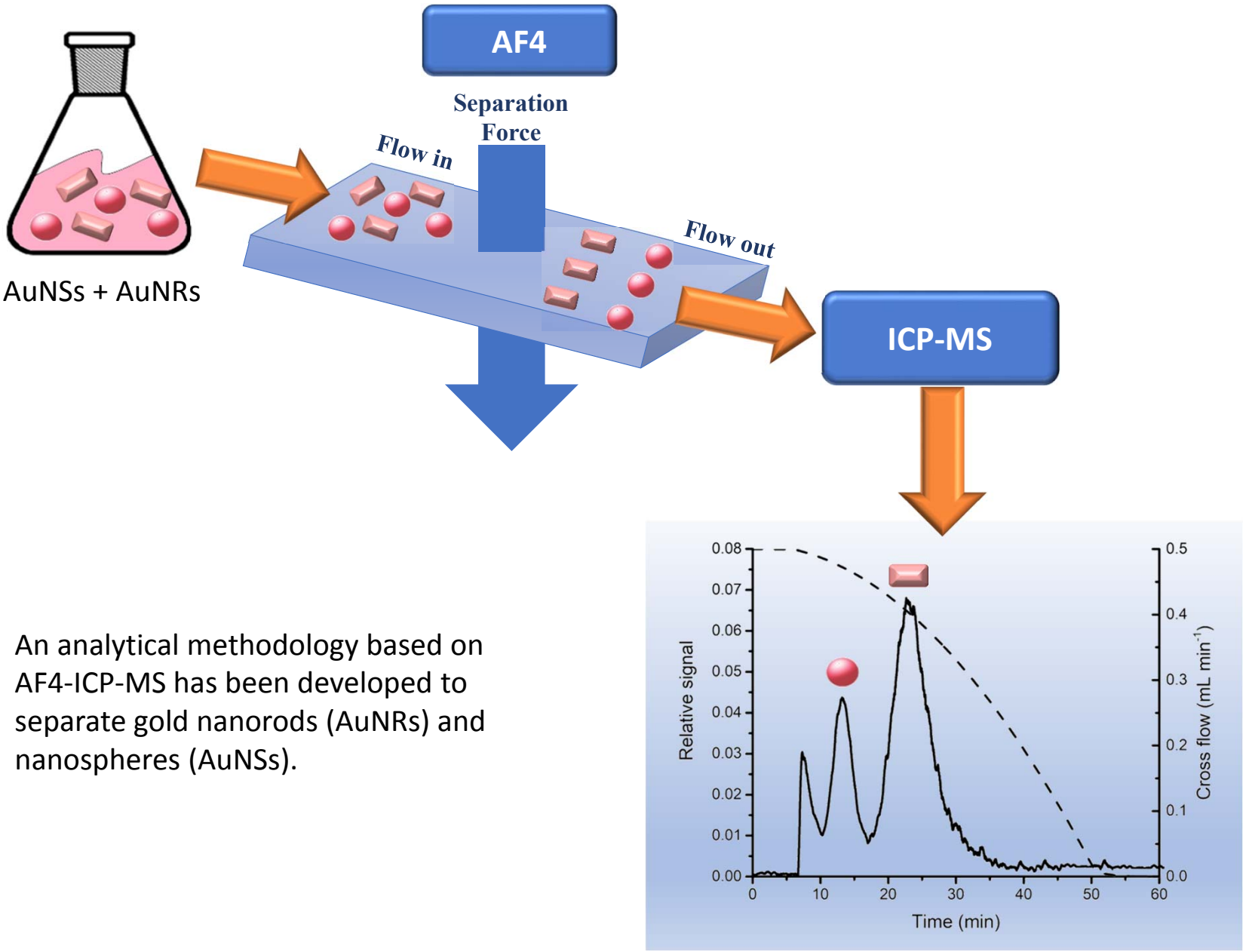

An analytical methodology based on AF4-ICP-MS has been developed to separate gold nanorods (AuNRs) and nanospheres (AuNSs).

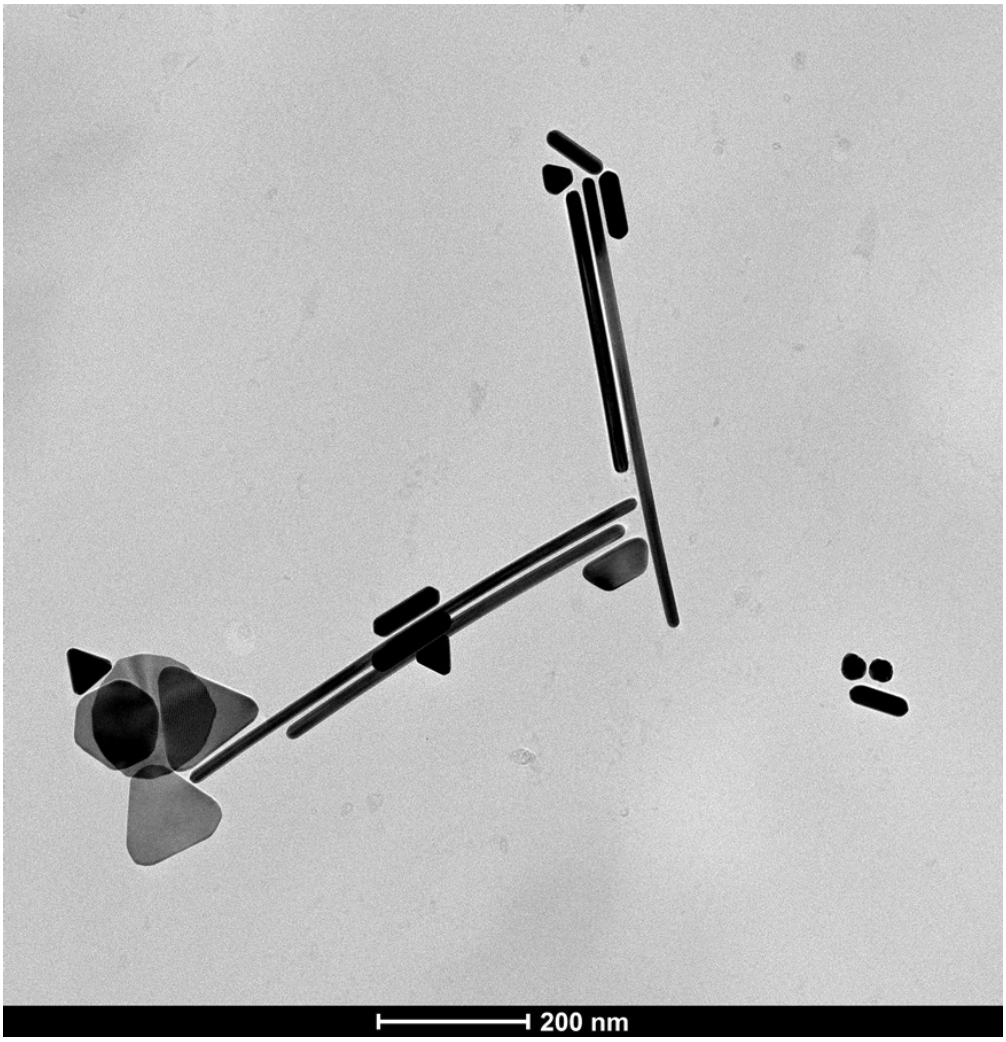

Figure 5. TEM image of a sample obtained in the synthesis procedure of 4.6 aspect ratio AuNRs (dilution 1/100).

184x190mm (120 x 120 DPI)